Title

"Integrated Structured Light Architectures" — A Review

Author

Durrani, Arman

Publication Date

2023-10-01

“Integrated Structured Light Architectures” – A Review

Arman Durrani

Undergraduate electrical engineering student of the University of California, Los Angeles (2020-2024)
adurrani@g.ucla.edu

Abstract : The goal of this paper is to validate the work done in “Integrated Structured Light Architectures” by analyzing and comparing the expected intensity distribution calculations with the retrieved phase distribution of the prototype.

INTRODUCTION

“Integrated Structured Light Architectures” presents a generalized laser architecture along with an experimental demonstration of the architecture’s usability.

The proof-of-concept architecture consists of seven fiber-based beamlines each split from a femtosecond mode-locked laser operating at the C-band telecom wavelength range in addition to a control beamline. Each of the beamlines is phase-locked to one absolute reference phase; however, each of the seven beamlines' field parameters undergo some kind of user based manipulation and monitoring. In addition, each beamline contains a phase modulator that imposes a phase relationship with respect to the reference beamline phase via an FPGA. The intensity and polarization vector control units for each beamline are a half waveplate, polarizing beam splitter, and quarter waveplate placed on a fiber pigtailed delay stage. After individual manipulation of the field vectors, circularly birefringent fibers preserve each beamline’s final polarization state prior to synthesis. Thus is formed a laser architecture that can deliver programmable laser pulses in the form of a free-space synthesized light bullet.

As for the demonstration, a soliton mode-locked Er:Yb:glass laser oscillator is used with CEP stabilization based on a feed-forward system. The oscillator delivers 140 mW of power in 175 fs pulses at a repetition rate of 204 MHz with a spectral bandwidth of 14.9 nm centered around 1.55 µm. The light from the oscillator is then split into two beamlines, one towards the in loop feedback measurement and the other through an acoustic-optic frequency shifter and towards the outer loop. Both beamlines are coupled into stretcher fiber which is spliced with Er:fiber amplifiers. The pulse is then recompressed and undergoes octave spanning. After, it is passed through a series of bandpass filters centered at 1024 nm and focused into an avalanche photodiode. The raw signal is then filtered to isolate the carrier envelope offset frequency which is then mixed by a local oscillator and amplified to 26 dBm.

The figure below shows the demonstration results of generating far field complex phase and intensity distributions given a near-field hexagonal arrangement of seven identical beams that have no discernable differences except for their amplitudes (turned on or off) and phase differences from the control beam.

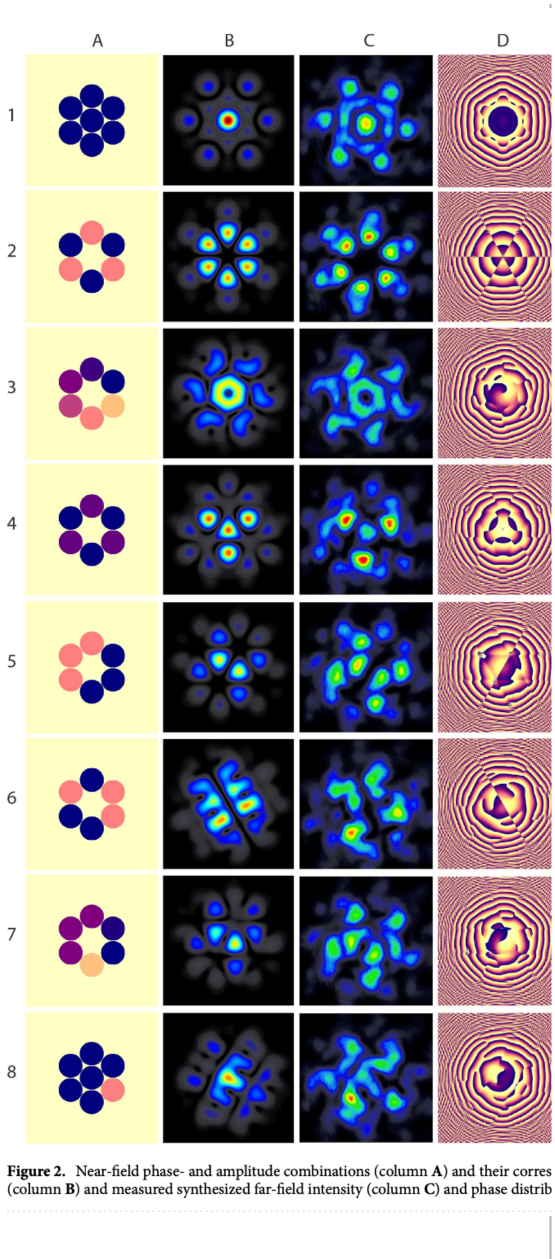

Figure 1 : Near field phase and amplitude combinations (column A) and their corresponding retrieved (column B) and measured synthesized far-field intensity (column C) and phase distributions (column D)

Given the information provided in regards to the architecture and the experimental data gathered from the demonstration, the intensity profiles for the first three near-field arrangements will be replicated as closely as possible

KEY ASSUMPTIONS & METHODOLOGY

In order to replicate the results shown above, we start by assuming that the distributions can be considered to be Laguerre-Gaussian in nature. This assumption is valid considering that the paper states the far field distributions are Laguerre Gauss / helical shapes, directly implying that the input distributions must be Laguerre-Gaussian as well, as this is a requirement for a Laguerre Gauss output distribution.We then further make assumptions about the medium that the experiment is conducted in to form the basis of the equations that will govern the system. We assume that the medium is transversely isotropic and homogeneous with no structural symmetry. Moreover, the following Laguerre-Gaussian intensity distribution chart is used as a basis for the interpretation of experimental results :

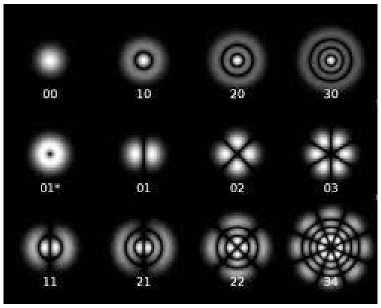

Figure 2 : Laguerre-Gaussian mode distributions

RESULTS AND INTERPRETATION

Before venturing into specifics amongst the three distributions, it is important to notice that there is an immediately observable baseline correctness in the calculated distributions (column two of the figure above). For a Gaussian beam, it is known that the intensity is given by

$$\textbf{Equation 1} : I(z, r) = I_0(z)exp(-\frac{2r^2}{w^2(z)})$$

given that w is the waist band size, r is the beam center radius, and z is the distance from the origin of the light source. Considering that these parameters are identical among the beamlines in this demonstration, this means that the transverse intensity distribution collected at any value z, should show equivalent intensities for each of the beams. And in the case of the demonstration, we see in the calculated far field intensity distributions that the intensities of each of the beams is nearly identical, supporting this baseline criterion for correctness. For the sake of simplicity in our analyses, let us assume that the normalized intensity for the sample input patterns is 1 and that the half-beam diameter drops by a factor of $1/e^2$ by the time the far field distribution measurement is taken. We will also assume that the Gaussian beam radius falls by about 1/e.

Now, let's take a closer look into each pattern and the prototype's resulting intensity distributions. In the first distribution, we see that we have seven beams in total that are all identical in amplitude and phase. We then see the following intensity distribution. (Left is input pattern, right is far field distribution)

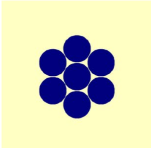

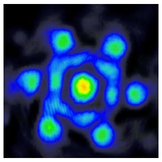

Due to the fact that in this example, each beam is identical, it logically follows that the resultant pattern is fully rotationally symmetric. Given that in our We expect the intensity patterns of each of the outer beams to look identical, which is directly observed by the symmetry of the output pattern and the fact that each of the circular peripherals in the output are of equivalent intensity. Using Equation 1, we see that the intensity at any point r in the far field distribution is still proportional to the corresponding intensity at points r in the input pattern by a factor that is determined by the exponential term

$exp(-\frac{2r^2}{w^2(z)})$. Moreover, we see that the radii of the beams seems to have indeed fallen by around a factor of 1/e. This seems to be the case across each of the 3 samples in this paper analysis.

For the second distribution, we have six beams now, with the center beam removed. The top and bottom right and left beams are off phase by π. (Left is input pattern, right is far field distribution)

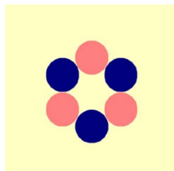

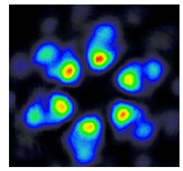

Once again we see that the intensity distributions are the same for each beamline, and we know this to be true due to the proportional relationship established in equation 1. Because the beamlines are off phase by exactly π, assuming a periodicity of 2π, it makes sense that the intensity profiles of each of these beams once again match in pattern, and we see that the intensities of each of these circular patterns is the same. The center is hollow which is again in line with a Laguerre-Gaussian distribution of higher order. As stated earlier, the beam width and beam radius degradation is in line with our assumptions.

For the third and last distribution, there is once again six beams, however each beam is slightly off phase from its neighbors. (Left is input pattern, right is far field distribution)

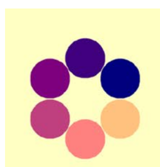

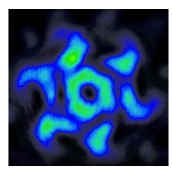

We see that the result is quite an interesting intensity distribution. The middle of the intensity distribution is a hollow circle which is expected once again considering the established basis of Laguerre-Gaussian intensity distributions. The sickle cell shape of the surrounding seems to be tilted slightly counterclockwise which is expected due to the fact that the beams are all identical however their phase changes slightly counterclockwise. We also see the center circle is hollow which is in line with what is expected from a Laguerre-Gaussian distribution. Thus, the calculated pattern is qualitatively in line with what is expected. Moreover, since the beam width and beam radius degradation is in line with our assumptions from earlier, we can say that these results are in line with our expectations quantitatively as well.

CONCLUSIONS & CRITIQUES

In short, the prototype's generated far field intensity profiles match up with the expected distributions. It should be said that quantitative analysis for this experiment was rather difficult because the amplitude and phase differences were displayed in static graphs; i.e. there were no data points quantitatively analyzed in the paper, so no calculations could be replicated to ensure that certain data points in particular matched our expectations. Had the paper analyzed certain points in the distributions, the findings may have been clearer to the reader and more replicable.

REFERENCES

1. *Lemons, R., Liu, W., Frisch, J. C., Fry, A., Robinson, J., Smith, S. R., & Carbajo, S. (2021). Integrated structured light architectures [Scientific Report]*
2. *Pampaloni, F.; Enderlein, J. (2004). "Gaussian, Hermite-Gaussian, and Laguerre-Gaussian beams: A primer". arXiv:physics/0410021*
3. *Vallone, G. (April 8, 2015). "On the properties of circular beams: normalization, Laguerre–Gauss expansion, and free-space divergence". Optics Letters.* ***40*** *(8): 1717–1720. arXiv:1501.07062.*
4. *Lemons,R.&Carbajo,S.Coherentopticspropagationandmodeling.https://github.com/slaclab/CCPM/tree/1.0.0%0A*